RESEARCH ARTICLE

Design, Development and Optimization of Solid Lipid Nanoparticles for Ocular Delivery of an Antifungal Agent

Raffah K. Mahal*, Fatima Al-Gawhari

College of Pharmacy, University of Baghdad, Baghdad, Iraq

Received: 22nd December, 2022; Revised: 07th January, 2023; Accepted: 20th February, 2023; Available Online: 25th March, 2023

ABSTRACT

Oral and intravenous dosing of the second-generation antifungal drug voriconazole (VCZ), with its wide range of antifungal action, is commercially accessible. Visual and hepatic problems might occur when VCZ is used in large doses. Voriconazole SLNs were prepared in this study with the goal of increasing corneal penetration and drug release. The thin film hydration approach was used to make VCZ SLNs. The central composite experimental design was used to maximize the impacts of independent processing factors on vesicle size (R1), drug entrapment efficiency (%EE) and zeta potential (ZP; R3) responses on lipid concentration (X1), surfactant concentration (X2), and sonication duration (X3). An evaluation of the drug release profile, corneal penetration, antifungal susceptibility, and cytotoxicity of the improved formula was conducted. The improved recipe achieved the best results with a ZP of -39.6 ± 0.28 mV, an average particle size of 156 ± 3.84 nm, and an EE% of 89.2 ± 2.01. When compared to the unformulated drug solution, the VCZ-SLNs had a prolonged 10 hours drug release profile with improved corneal penetration, with P_{app} and J_{ss} measuring 14.35×10^{-2} cm h^{-1} and 4.61 mol h^{-1}, respectively, instead of 7.28×10^{-2} cm h^{-1} and 2.48 mol h^{-1}. Non-irritating VCZ-SLNs were determined to be corneal tissue, according to the study. Improved corneal penetration and higher antifungal activity without harmful effects on ocular tissues were achieved by VCZ-SLNs.

Keywords: Antifungal, Central composite design, Permeability coefficient, Solid lipid nanoparticles.

International Journal of Drug Delivery Technology (2023); DOI: 10.25258/ijddt.13.1.54

How to cite this article: Mahal RK, Al-Gawhari F. Design, Development and Optimization of Solid Lipid Nanoparticles for Ocular Delivery of an Antifungal Agent. International Journal of Drug Delivery Technology. 2023;13(1):327-339.

Source of support: Nil.

Conflict of interest: None

INTRODUCTION

Ophthalmic drug delivery has used nanostructured systems such as solid lipid nanoparticles (SLNs). These have improved the bioavailability of poorly soluble drugs, while decreasing the applied dosage and toxicity of the pharmaceuticals.[1] Nanotechnology-based formulations using SLNs may offer a continuous and regulated release of medications, avoiding the frequent applications connected to conventional delivery methods.[2] In addition to these advantages, nanomedicines have a number of other advantages, including the ability to prepare modified eye drops that can be self-instilled, the elimination of the need for repeated application, and the creation of a shielding barricade against metabolic enzymes on the eye surface.[3] Because these particles are so small, they have no effect on ocular vision.[4]

There are many advantages to using SLNs over other colloidal carriers, such as the ability to control the release of drugs and to target them, as well as the stability and loading of drugs (hydrophilic and lipophilic), the absence of biotoxicity due to the use of physiological lipids, and the ease of scaling up *via* autoclaving.[5-8] Ocular SLNs systems have been shown to be more stable than aqueous eye drops in terms of ocular surface and conjunctival sac retention, resulting in continuous release of the medication.[9-11] The lipophilic properties of SLNs would allow the drug molecules contained in SLNs to easily permeate the epithelium. Many antiphlogistic drugs, including diclofenac, ibuprofen, piroxicam, and indomethacin, have been effectively administered to the eye utilizing SLNs as carriers.[12-14]

One of the most interesting and promising scientific fields today is the creation of improved.[15] Therapeutically effective, ocular delivery systems with improved corneal penetration, prolonged ocular residence time, and improved mucoadhesive properties while maintaining high patient compliance at a low cost.[16] By producing colloidal drug delivery systems with particle sizes between 1 and 1,000 nm, Nanotechnology may be used to generate new medicines and improve existing treatment methods. In contrast to colloidal carriers, SLNs, constituted of physiologically acceptable solid lipids distributed in an aqueous surfactant solution in the range of 100–150 nm, are a viable alternative. High drug loading, high stability with little drug leakage, minimal physiological toxicity, controlled

**Author for Correspondence: Dr.rafahkh@gmail.com*

and/or prolonged drug release, drug targeting, and large-scale manufacturing adaptability are just a few of the numerous benefits of using these devices.[17-20] Their lipophilic nature and tiny particle size allow them to penetrate physiological barriers more effectively than larger particles. With its mucoadhesive and sterilization tolerance, SLNs are a very effective ocular drug delivery method with higher corneal absorption, increased ocular bioavailability, longer ocular retention duration, and a sustained release profile without affecting vision.[21-23]

At pH 1.2, Voriconazole (VCZ) is a lipophilic drug with maximal solubility of 2.7 mg/mL. Solid lipid formulations containing VCZ have been developed to increase VCZ's intraocular accessibility.[24] Yeast or fungal infections are treated with VCZ, an antifungal medication. Inhibiting 14 alpha-lanosterol demethylation, a key step in fungal ergosterol production, VCZ binds and inhibits ergosterol synthesis.[25] Ergosterol loss in the fungal cell wall is associated with the build-up of 14 alpha-methyl sterols, which might explain the antifungal action. VCZ is available in powder for infusion, oral solution, and tablet form on the market. As a result, the present research sought to create and assess a topical eye solution based on VCZ loaded-SLNs. Research also sought to evaluate clinically the effectiveness of a topical antifungal formulation presently on the market for treating patients with candidiasis with a produced VCZ-SLNs solution.[26]

MATERIALS AND METHODS

Sigma-Aldrich Co. bought VCZ (St Louis, MO, USA). Gattefosse SAS sent Precirol ATO 5®, Gelucire 50/13®, Transcutol P®, and Compritol 888® as gifts (Saint-Priest Cedex, France). All of the ingredients were acquired from EMD Millipore, including Kolliphor, Solutol HS 15, Pluronic f68, glyceryl monostearate, stearic acid and palmitic acid, cetostearyl alcohol and stearyl amine (Billerica, MA, USA). Sigma-Aldrich Co. provided all HPLC grade solvents procured and utilized without further purification.

Animals

We obtained New Zealand white rabbits from the Anurag University School of Pharmacy's Center for Nanomedicine animal home. It was approved by the Institutional Animal Ethics Committee (IAEC). Six New Zealand white rabbits weighing 1–1.5 kg were randomly divided into two groups of three each. An animal house in an institutional setting provided the animals with unfettered access to food and water.

Screening of Solid Lipid Materials

Tests were conducted on the solubility of VCZ-SLNs lipid cores, such as Compritol 888 and Precirol ATO 5®, as well as palmitic acid, stearic acid, cetostearyl alcohol and tristearin.

Determination of VCZ Lipid Solubility

Measurement of drug partitioning behavior between an aqueous solution and the tested lipid using Joshi and Patravale's modified approach[27] demonstrated the solubility of VCZ in many distinct types of solid lipids. For this experiment, 10 mg of VCZ was dissolved in 10 mL of a water/lipid combination and agitated for an hour in a 70°C water bath. Centrifugation at 15,000 rpm for 15 minutes separated the aqueous layer after allowing the mixture to settle to ambient temperature. We collected the aqueous layer and used an HPLC technique to determine the VCZ content.[28] By subtracting the concentration of the aqueous layer from the total quantity of drug added, the VCZ lipid solubility was computed and represented in percentage form.

Selection of Surfactant (Surface Active Agent)

An aqueous surfactant solution (3%) was heated to 70°C and combined with a set quantity of the chosen molten solid lipid (4%) to determine the best surfactant to employ in the production of VCZ-SLNs. For 5 minutes, the mixture was vortexed, then sonicated for 2 minutes. Vesicle size (nm), zeta potential (ZP) (mV), and polydispersity index (PDI) were measured after the mixture was quickly chilled in an ice bath. Precipitation was visually evaluated under suitable illumination after preparation and overnight storage at room temperature. The outcomes were tallied and compared.

Preparation of SLNs

The film hydration approach was used to make nano lipids. In a round-bottom flask, the lip and surfactant were dissolved in dichloromethane and methanol (a volatile organic solvent). For 45 minutes, the rotary evaporator was rotating at 60°C. A thin layer of lipid was deposited on the rotary flash evaporator's inner wall to remove the organic solvent and heated to 60°C before the organic solvent evaporated.[29] After 30 minutes of sonication, the aqueous phase containing VCZ was gently introduced to the flask with occasional shaking. Place the micro lipid solution in the fridge to cool down. Table 1 shows the nano lipid's chemical makeup.

Experimental Design

Preparing VCZ-SLNs was made easier with the use of a statistical design that included a central composite of three levels and three factors (Design Expert, Version 12.0.3.0, Stat-Ease Inc. Selected as independent variables are the solid lipid content (X1), the amount of surfactant (X2), and the frequency of sonication (X3). Table 1 summarizes the three layers of independent variables and response limitations. As outlined in the proposed experimental design and considering the main, interaction, and quadratic effects of selected independent variables on the prepared VCZ-SLNs formulae, a matrix of 20 runs was constructed to represent the observed response *via*, including three vesicles of various sizes (R1, R2, and R3) as well as the ZP. These ZP matrices were then evaluated for the observed response (Table 2). Several polynomial equations were created as a result of fitting the gathered response values to linear, two-factor interaction (2FI), cubic, and quadratic models for optimization. According to the program, the best model had greater coefficients of determination and a higher significance value at the selected probability level. The ANOVA feature of the program was used to validate

Table 1: Box–Behnken design formulation variables and their values

Constraints			
Independent factors			
Name	Low (-1)	Medium (0)	High (+1)
X1: Lipid (mg)	50	225	400
X2: Surfactant (^{o}C)	2.5	11.5	20
X2: Sonication time	2	4	6
Dependent variables			
Entrapment Efficiency (%)	Maximize	89.2 ± 2.01	
Vesicle Size (nm)	Minimize	156 ± 3.84	
Zetapotential	In range	-39.6 ± 0.28	
PDI	Minimize	0.188 ± 0.05	

Table 2: Observed responses to a central composite experimental design

Run	*X1*	*X2*	*X3*	*Y1*	*Y2*	*Y3*	*Y4*
1	519.3	11.25	4	55.2 ± 0.09	360 ± 2.51	-23.9 ± 0.38	0.395 ± 0.01
2	50	20	6	49.2 ± 1.23	324 ± 5.61	-26.5 ± 0.64	0.391 ± 0.03
3	50	2.5	6	89.2 ± 2.01	156 ± 3.84	-39.6 ± 0.28	0.188 ± 0.05
4	225	11.25	4	59.3 ± 0.12	325 ± 2.13	-24.2 ± 0.19	0.352 ± 0.13
5	225	-3.46	4	65.9 ± 0.94	389 ± 3.46	-26.7 ± 0.25	0.361 ± 0.21
6	-69.3	11.25	4	71.6 ± 0.68	198 ± 5.19	-36.4 ± 0.34	0.238 ± 0.11
7	50	2.5	2	80.3 ± 0.28	184 ± 7.26	-34.9 ± 0.26	0.243 ± 0.03
8	50	20	2	76.3 ± 0.61	283 ± 3.46	-29.1 ± 0.17	0.264 ± 0.23
9	225	11.25	4	60.2 ± 1.02	325 ± 1.28	-25.6 ± 0.81	0.352 ± 0.04
10	225	11.25	4	60.1 ± 0.59	325 ± 3.24	-25.9 ± 0.64	0.352 ± 0.51
11	400	20	2	76.4 ± 0.16	243 ± 5.24	-28.1 ± 0.29	0.249 ± 0.26
12	400	2.5	2	60.3 ± 0.27	315 ± 4.23	-23.7 ± 0.83	0.372 ± 0.13
13	225	11.25	4	61.2 ± 0.64	325 ± 2.06	-25.8 ± 0.94	0.352 ± 0.64
14	225	11.25	4	61.8 ± 1.07	325 ± 3.12	-25.9 ± 0.67	0.352 ± 0.28
15	225	25.96	4	54.2 ± 0.64	425 ± 5.24	-22.5 ± 0.85	0.412 ± 0.01
16	400	2.5	6	69.8 ± 0.28	394 ± 1.32	-24.3 ± 0.16	0.366 ± 0.03
17	225	11.25	0.63	80.6 ± 0.61	213 ± 5.03	-28.9 ± 0.35	0.243 ± 0.05
18	225	11.25	4	60.8 ± 0.84	330 ± 5.16	-25.9 ± 0.43	0.352 ± 0.06
19	225	11.25	7.36	75.9 ± 0.93	246 ± 4.18	-34.6 ± 0.62	0.296 ± 0.42
20	400	20	6	55.9 ± 0.27	384 ± 2.13	-24.1 ± 0.84	0.415 ± 0.12

the produced mathematical polynomial equations. Further investigation was done by creating three-dimensional (3D) surface and perturbation graphs.

$$y0=b0+b1X1+b2X2+b3X3+b12X12+b13X13+b23X2X3+b11X2X1\ldots.1$$

When Y0 is used as the dependent variable, the intercept is b0, and the regression coefficients are denoted by b1–b33.

Validation of the Experimental Method

The numerical prediction optimization function of Design Expert Software was used to verify the optimization approach based on the restrictions suggested by the three replies. The two VCZ-SLNs formulas were optimized based on the computed desirability as checkpoints. The hypothesized ideal composition was followed in the preparation of the formulations, which were then evaluated for a variety of reactions. Prediction errors (percentage) were computed by comparing observed values to expected values.

Lyophilization

Mannitol, a cryoprotectant, was added to the above-prepared aqueous dispersions, which were subsequently lyophilized for 24 hours to ensure physical stability and redisperability.[30] First, the liquid was prefrozen at 74°C, with a pressure of 0.02 mmHg, and the vials were placed in an adaptor. Freezing the dispersion and then drying it in a freeze-drier (Allied Frost's Lyophilizer FD-5-3 in New Delhi, India) produced a free-flowing powder of VCZ-SLNs after fitting the adapter into the machine.[31]

Table 3: Evaluation of primary VCZ-SLNs prepared for the selection of appropriate surfactant

Solid Lipid	*Surfactant*	*VS*	*ZP*	*PDI*	*Physical examination*	
					AP	*OS*
	Tween 20	359	-15.6	0.435	SP	P
	Tween 80	156	-39.6	0.188	NO	NO
	Cremophor RH 40	594	-13.5	0.649	P	P
Tristearin	Kolliphor EL	468	-25.7	0.469	SP	SP
	Solutol HS 15	368	-26.9	0.354	SP	P
	Pluronic f68	267	-31.5	0.284	No	SP
	Transcutol P	635	-16.2	0.529	P	P

P, precipitation; SP, slight precipitation; NP, no precipitation; PDI, polydispersity index; VS, Vesicle size; ZP, Zeta potential; AP. After preparation; OS, Overnight storage.

Table 4: Results of regression analysis and ANOVA for the response surface quadratic model

Formula	*VCZ-SLNs*			*SD*	*CV%*	*Adeq.*	*Remark*
	R^2	*Ad.* R^2	*Pr.* R^2				
Entrapment Efficiency (R^1)							
Linear	0.2967	0.1648	-0.2381	9.76			
2FI	0.6742	0.5238	0.1557	7.37			
Quadratic	0.9766	0.9555	0.8303	2.25	3.40	23.259	Suggested
Cubic	0.9921	0.9748	-0.3518	1.69			Aliased
Vesicle Size (R^2)							
Linear	0.4004	0.2880	-0.0817	63.10			
2FI	0.6144	0.4364	0.1290	56.14			
Quadratic	0.9730	0.9486	0.7962	16.95	5.59	22.1248	Suggested
Cubic	0.9895	0.9667	-1.2775	13.65			Aliased
PDI (R^3)							
Linear	0.4514	0.3485	0.0138	0.0537			
2FI	0.7815	0.6806	0.4419	0.0376			
Quadratic	0.9862	0.9739	0.8986	0.0108	3.27	30.246	Suggested
Cubic	0.9910	0.9716	-0.8718	0.0112			Aliased

Note: Underlined entries refer to "the best fit model terms". **Abbreviation:** CV%, coefficient of variation

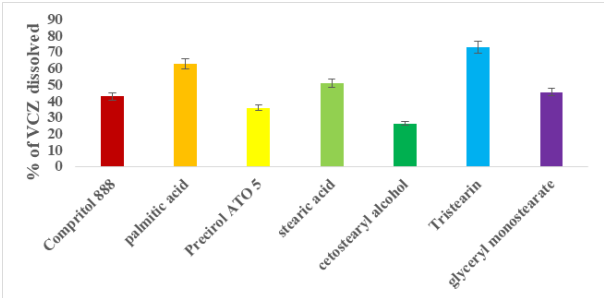

Figure 1: Solubility studies of solid lipid in VCZ.

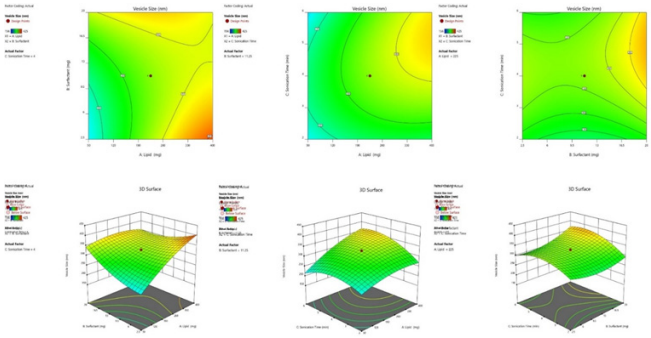

Figure 2: Counter and response surface plots of vesicle size against independent variables.

Characterization of SLNs

Particle Size and ZP Analysis

Ultrasonic dispersion of SLNs in distilled water for 30 s was produced. By using a Zetasizer Nano ZS-90 (Malvern Instruments, Worcestershire, UK) linked to the DTS software, the aqueous suspension of VCZ-loaded nanoparticles was characterized in terms of the average particle size (z average), ZP, and polydispersity index (PDI). Using a malvern zetasizer 4 (Nano ZS, Zen 3600) at 25°C and appropriate dilution with double distilled water to a sufficient intensity, the particle surface charge (ZP) was calculated.[32] At a minimum, three independent measurements were made for each parameter. It was essential that the pH of the samples be kept between 7.0 and 7.5 at all times.

Entrapment Efficiency Percentages (EE%) and Drug Content Measurements

For 30 minutes, the freeze-dried SLNs were heated at 70°C in securely capped glass vials, which were then put in a deep freezer (18°C) in order to precipitate the lipid, resulting in the medication remaining in the supernatant, while the lipid was removed. 20 minutes at 11 200 × *g* ultracentrifugation was used.[33] At a wavelength of 256 nm, a UV-visible spectrophotometer analysed the supernatant for the presence of VCZ. Using distilled water (5 mL), 25 mg of the lipid nanoparticles formulation was dissolved in order to quantify the amount of unentrapped drug. The nanosuspension was then centrifuged at 25, 200 × g for 30 minutes at 4°C in an ultracentrifuge. An ultraviolet-visible spectrophotometer reading of 256 nm was used to check the supernatant for the presence of VCZ. Excess supernatant content was subtracted from the total concentration used to manufacture the nanoparticles to determine how much of the medication encapsulated in the particles was present. This equation was used to compute the percentage entrapment efficiency (EE):

$$Entrapment\ Efficiency = \frac{Total\ amount\ of\ drug\ loaded - free\ drug\ amount}{Total\ amount\ of\ drug\ loaded}$$

In order to determine the drug concentration and loading in VCZ-SLNs, the lipid precipitation method was used. First, SLNs and SLNs-eye solution (0.1 mL) were precipitated with 0.9 mL of methanol before centrifugation at 13,000 rpm for 15 minutes and HPLC analysis of the supernatant.

Drug loading in SLNs were calculated using following formula:

Drug loading (%) = $(Wt.-Wu/W_L) \times 100$ ---------- (1)

Weight of the unentrapped medication is Wt. weight of the lipids is WL and the sum of these three components is Wt.

Particle Morphology (TEM)

Particle morphology was seen using a transmission electron microscope TEM. In this experiment, we used a 10 µL sample that was put on the grids and left to stand for 90 seconds at room temperature. Filter paper was used to eliminate any extra liquids. The TEM was used to investigate all samples at an acceleration voltage of 100 kV.[34]

Surface Morphology (SEM)

Visualizing surface morphology was done using a scanning electron microscope SEM. A double-adhesive tape was used to stick an aluminum stub on which the SLNs powder was softly sprinkled. This research used an electron microscope with an accelerator of 30kV (LEO 435 VP from Eindhoven, Netherlands) to investigate all materials.

Fourier-Transform Infrared Spectroscopy (FTIR)

FTIR spectroscopy was used to acquire the spectra of VCZ, Tristearin, Tween 80, and their physical combination that corresponds to the optimum formula, as well as freeze-dried F3 and its plain SLNs (Thermo Fisher Scientific iS10 Nicolet). Potassium bromide was used to integrate small quantities (2 mg). They were first crushed into fine powder using a hydrostatic press and then formed into KBr disks. From 500 to 4,000 cm^{-1} was the scanning range.

Differential Scanning Calorimetry (DSC)

There will be about 10 mg of each of the following: VCZ, tristearin, and physical mixes with the same ratio as the selected formula. All samples were kept in standard aluminium pans (Shimadzu DSC 50, Tokyo, Japan), heated at 10°C/min under a continuous dry nitrogen environment, and purged at a flow rate of 20 mL/min.[35]

RESULTS AND DISCUSSION

Selection of Solid Lipid and Surfactant

Lipid nanoparticles solubility is critical to the tolerability of SLNs formulations to a given drug.[36] The solubility of VCZ in several solid lipids was examined to enable the selection of a solid lipid ideal for preparing the SLNs formulation to optimize drug loading and EE. The materials and methods section describes the steps to determine how much drug is partitioned to the liquid fatty layer after being shaken with water. With percent drug partitioned values of 72.59 and 62.51%, tristearin and palmitic acid demonstrated greater VCZ solubilizing activity (Figure 1). Because tristearin and palmitic acid molecules are made up of mono, di, and triglyceride contents, they have loose, extremely porous structural properties.[37] This allows for better accommodation and increased solubility of the drug. A blend of palmitic acid and tristearin, tristearin's diverse fatty acid composition and looser structure explain why it was chosen to be the lipid core for synthesizing VCZ-SLNs in this work.[38]

Precipitation, particle size, ZP, and PDI were used to help narrow down the surfactant options. There were no symptoms of precipitation, as indicated in Table 3, for the Tween 80-based SLNs formula, which had the lowest VS (156 ± 3.84 nm), an acceptable ZP (-39.6 ± 0.28 mV), and an acceptable PDI (0.188 ± 0.05). As a result, Tween 80 was chosen as the best surfactant for making VCZ-SLNs formulations. The surfactant's hydrophilic/lipophilic balance (HLB) value heavily influences the vesicle size of SLNs formulations, with smaller particles being associated with larger HLB values.[39] In compared to other surfactants, Pluronic F68 has a high HLB value (HLB =15). This might explain the gathered data.

Statistical Analysis of Experimental Data

Experimental designs based on statistics enable multifactorial statistical analysis to select control variables that significantly affect a specified response with minimal process variation, strengthening the collected results and eliminating the need for further inspection.[40] There are fewer experiments required to derive polynomial equations when using the central composite design compared to other related statistical experimental tools. Central composite design was employed to investigate the influence on VCZ-SLNs formulae's properties of three various levels of solid lipid concentration (X1), surfactant concentration (X2), and sonication duration (R3). Using this matrix design, it can be shown in Table 2 that the independent variables chosen had a substantial impact on the observed responses. There were quadratic interactions between all three independent

Table 5: Coefficients of different formula variables according to the best-fit response surface model

Source	*R1*		*R1*		*R3*	
	f-value	*p-value*	*f-value*	*p-value*	*f-value*	*p-value*
Model	46.31	< 0.0001	39.98	< 0.0001	79.63	< 0.0001
A	52.25	< 0.0001	111.52	< 0.0001	213.07	< 0.0001
B	54.52	< 0.0001	15.37	0.0029	35.20	0.0001
C	19.86	0.0012	21.22	0.0010	79.71	< 0.0001
AB	52.57	< 0.0001	53.00	< 0.0001	96.01	< 0.0001
AC	1.28	0.2849	18.65	0.0015	8.37	0.0160
BC	107.28	< 0.0001	7.47	0.0211	135.48	< 0.0001
A^2	5.81	0.0367	21.02	0.0010	32.38	0.0002
B^2	0.1712	0.6878	30.82	0.0002	9.29	0.0123
C2	126.70	< 0.0001	72.33	< 0.0001	106.26	< 0.0001
Lack of Fit	11.86	0.0084	136.89	< 0.0001	27.32	0.0012

Note: *Significant model terms.

Table 6: Amount of MN permeated and retained in hairless rat skin from different formulations (tape stripping experiments)

Formulation	*Drug in tape strips (μg/cm²)*	*% Drug in skin after tape striping*
VCZ suspension	20.35.4 ± 2.95	11.36 ± 1.29
VCZ-SLNs	169.5 ± 6.23	89.56 ± 3.16

Table 7: Pharmacokinetic parameters of optimized formulation (F3)

Parameters	*Drug suspension*	*F3*	*Marketed formulation*
Intercept	2.27441	2.179937569	2.184446271
Slope	-0.0127819	-0.030567681	-0.012099664
C0 (mcg/mL)	188.1092	151.3343686	152.9136557
k (hr-1)	0.0294367	0.070397368	0.027865527
dose (mg)	10	10	10
dose (mcg)	1000	1000	1000
vd (mL)	53.16061	66.07884312	65.39638302
Vd (L)	0.0073733	0.066078843	0.065396383
t1/2 (hr)	23.542007	9.844117976	24.86943859
Clearence (l/h)	0.000217	0.004651777	0.001822305
AUC 0-t (μg.h/mL)	47.152301	37.95859214	38.35341394
AUC 1-t (μg.h/mL)	5287.5	1940.75	2902.75
AUC 1-inft (μg.h/mL)	2276.067	411.9472169	2691.497683
AUC tot (μg.h/mL)	7610.7193	2390.655809	5632.601096
C_{max} (μg/mL)	1978.2456	2851.3459	1571.86425
T_{max} (h)	1.20351	1.2436	1.02146

variables in the observed responses, with the maximum multiple correlations and adjusted coefficients and the expected sum of squares and significant statistical terms at the indicated probability level. In light of the low SD and strong agreement (difference 0.2) between the anticipated and adjusted R^2, the components investigated and the observed responses seem to have a nonlinear relationship, as shown in Table 4. Usually referred to as a noise signal, accuracy levels >4 that show a negligible influence of uncontrolled experimental conditions may be a substantial source of unpredictability.

The generated polynomial quadratic equations were tested using ANOVA. For each of the three answers, ANOVA indicated significant model F-values with a probability of less than one-hundredth of 1%, as shown in Table 5. There is only a 0.01% chance of noise. In line with the predicted suitable precision values, these findings demonstrate that the model equations provided for traversing the design space are appropriate.

Effect on Particle Size

The concentration of lipid/surfactant, homogenization conditions, and sonication duration and speed all influence the VS of SLNs. A quadratic regression equation may represent the quantitative interaction effects of the three factors on the measured VS, as shown in Table 2 and Figure 2. The generated

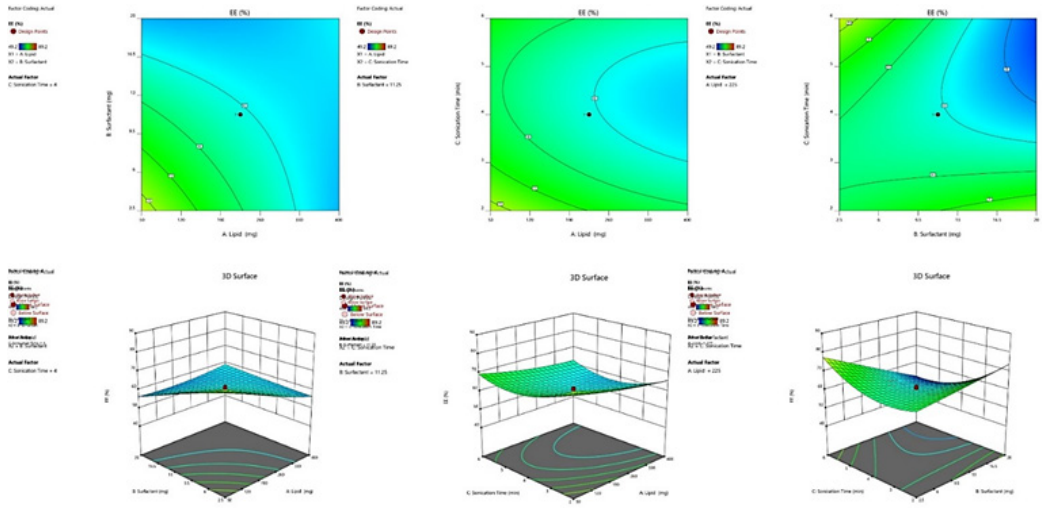

Figure 3: Counter and response surface plots of %Entrapment Efficiency against independent variables.

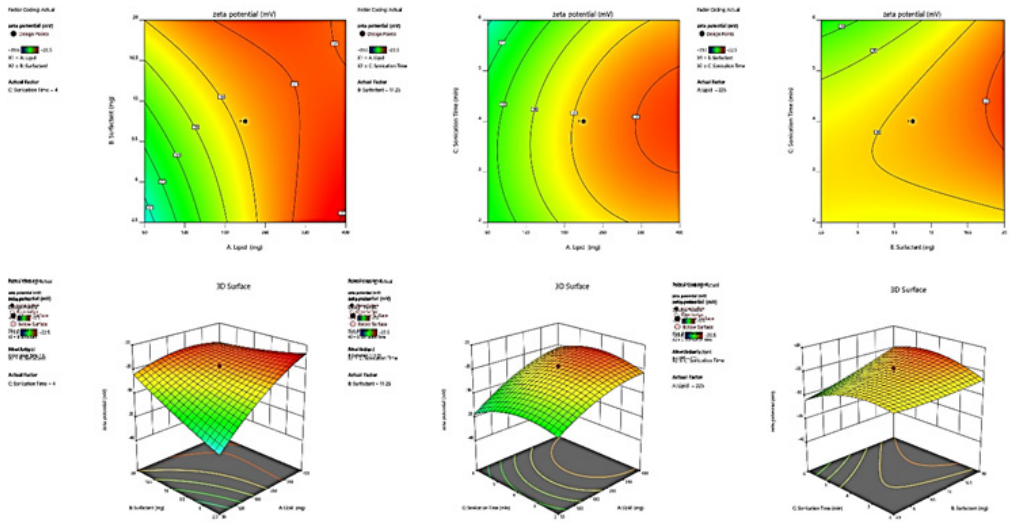

Figure 4: Counter and response surface plots of zeta potential against independent variables

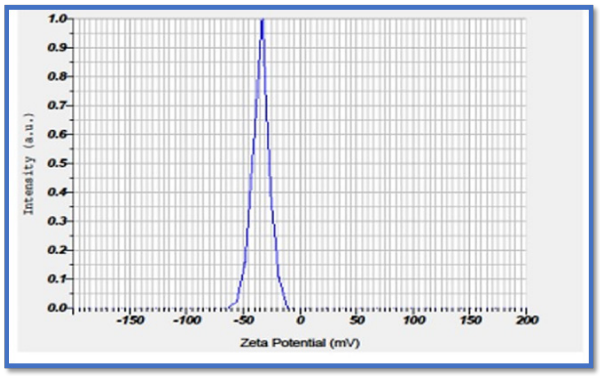

Figure 5: Zeta potential of optimized formulation.

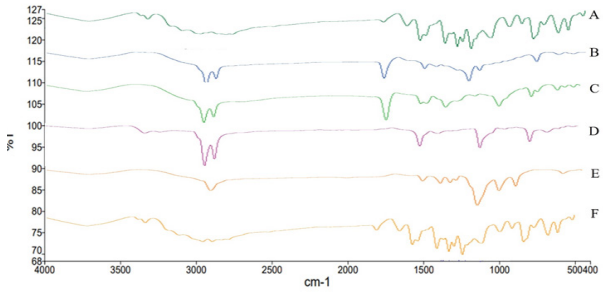

Figure 6: FTIR spectral studies of (A.) VCZ, (B.) Tristearin, (C.) Palmitic Acid, (D.) Stearyl Alcohol, (E.) Poloxamer 188 and (F.) optimized formulation.

VCZ-SLNs had a VS range of 156 ± 3.84 nm (F3) to 425 ± 5.24 (F15) nm.

EE= +60.51 -4.41A -4.50B -2.72C +5.77AB +0.9000AC -8.25BC +1.43A2 +0.2455B2 +6.68C2

Positive values suggest a synergistic impact, whereas negative values indicate an antagonistic effect. p >F0.05 shows significant model terms. However, only the model variables A^2, B^2 and C^2 were shown to have an influence on VS according

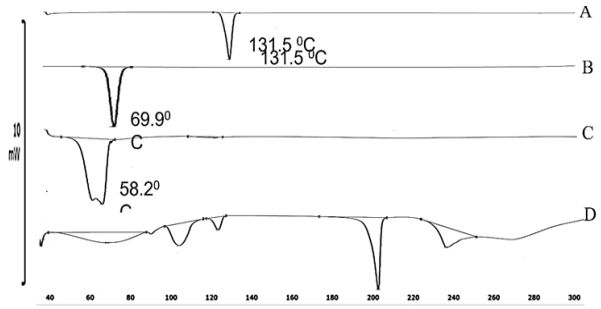

Figure 7: DSC studies of (A.) VCZ, (B.) Tristearin, (C.) Poloxamer 188, (D.) Optimized Formulation.

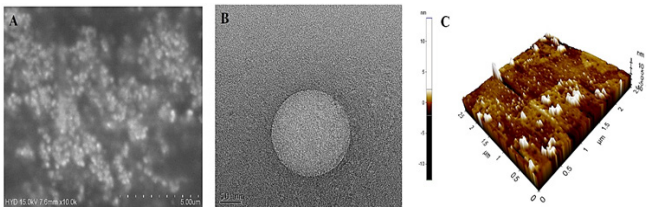

Figure 8: Morphological studies of (A.) SEM, (B.) TEM and (C.) AFM.

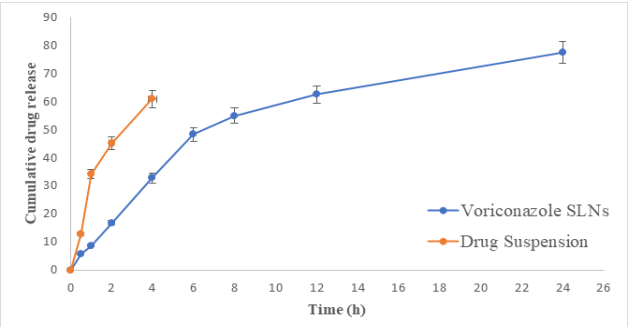

Figure 9: *In-vitro* release studies of VCZ suspension and VCZ SLNs.

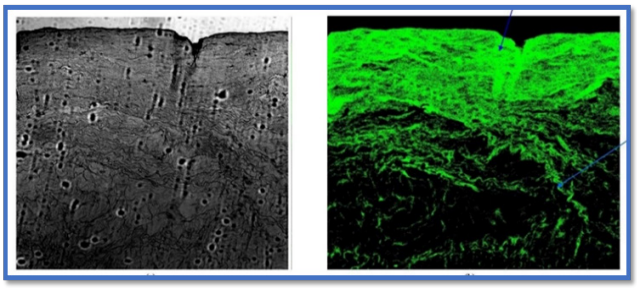

Figure 10: Corneal uptake pictures captured by CLSM. Fluorescent labelled Voriconazole SLNs (A) and non-fluorescent SLNs (B).

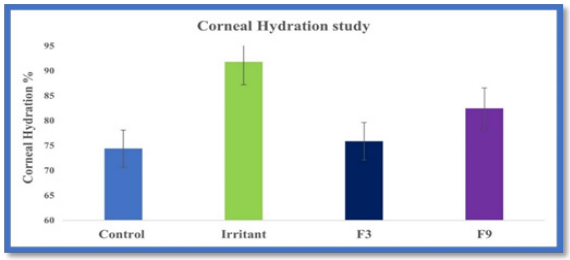

Figure 11: Voriconazole SLNs corneal hydration research (Mean SD, n=3) There is statistical significance (*p 0.05, as determined by the Dunnett multiple comparison test).

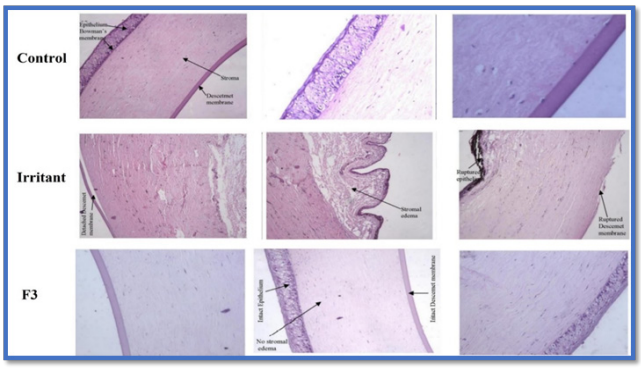

Figure 12: Histopathological studies of Control, and Irritant and VCZ-SLN isolated cornea's.

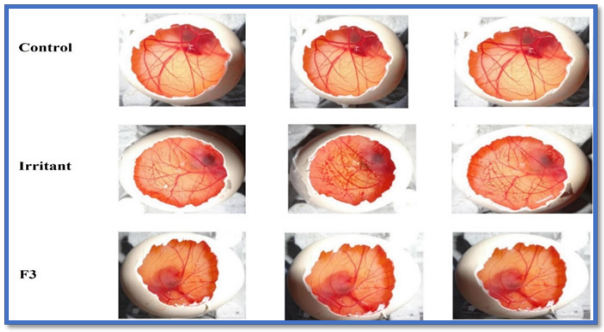

Figure 13: HET-CAM assay after treatment with (A) Control, (B) Irritant and (C) VCZ-SLN.

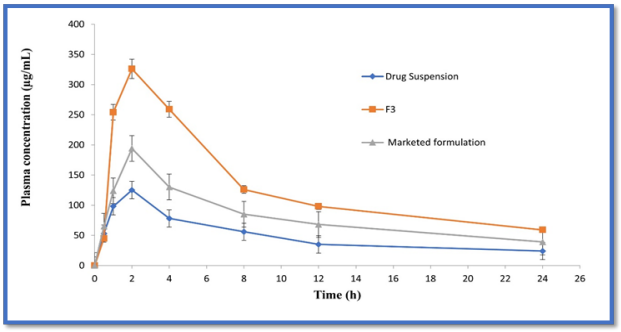

Figure 14: The AUC is shown after topical and suspension Voriconazole SLNs administration (Mean SD, n = 3). When analyzing data, a student t-test may tell us whether or not the findings are statistically significant (or not).

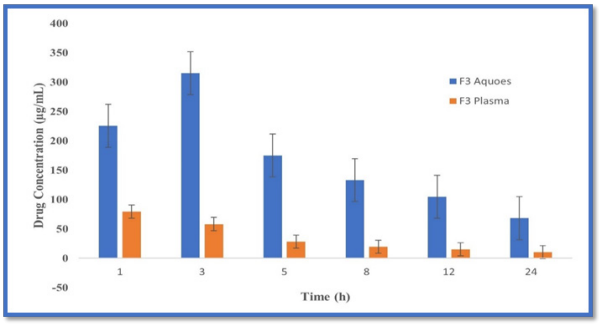

Figure 15: depicts the aqueous humor and plasma distribution of voriconazole after topical treatment of (A) voriconazole SLNs and/or (B) VCZ solution (Mean SD, n=3).

to the findings of the ANOVA. C^2 represents the interaction impact on VS when two variables are concurrently modified. A and B indicate the major effects of altering one variable at a time within its given constraint range. VS was substantially higher in F1, F5, F17, and F20 (X1=225-500 mg) than in F3 (X1=below 200 mg) at varying concentrations of solid lipid (X1), as seen in the data shown in Table 5. Solid lipid content rises with consecutive VS growth, which might account for the formula's increasing consistency and surface tension.[41] When X2 and X3 were held constant, F1, F5, F17, and F20 had much reduced VS than other formulations, correspondingly, when the surfactant concentration was increased. Nonlinear VS decreases of 248 to 156 nm were seen when the X1X2 and X2X3 interactions were taken into consideration. Because of the high shearing conditions used in the preparation process, the surfactant's influence on VS of SLNs formulations may be linked to the considerable reduction in surface tension and surface free energy (SFE) that occurred. VS was shown to be less affected by surfactant when sonication frequency was increased, which led to bigger increase in SFE and hence a less impact of surfactant on surface tension and VS. Synergetic quadratic effect of sonication frequency ($X3^2$) on VS, which has a significant model term. It supports the effect of an increased sonication frequency on SFE of the formula mixture, which results in a significant decrease in physical stability as the internal phase tends to aggregate[42] spontaneously. The insignificant coefficient terms show that simultaneous modifications to X3 and X1 had a minor impact on VS. VS was found to be most strongly influenced by lipid content (X1), with an exponent of 9.66, whereas X2X3 had the least effect on VS when the coefficient values of important model variables were compared. Lipid concentration (X1) was shown to be the most significant factor in altering VS, as demonstrated by the construction of a perturbation plot.

Effects on EE

For various factor levels, the %EE varied from 49.2 ± 1.23 (F2) to 89.2 ± 2.01% (F3), as shown in Table 2. The following is the derived polynomial quadratic equation for the EE.

$$EE = +60.51 -4.41A -4.50B -2.72C +5.77AB +0.9000AC -8.25BC +1.43A^2 +0.2455 B^2 +6.68 C^2$$

Table 5 shows that the following model terms are all significant with p>F0.05: A, B, C, AB, BC, A^2 and C^2. There were

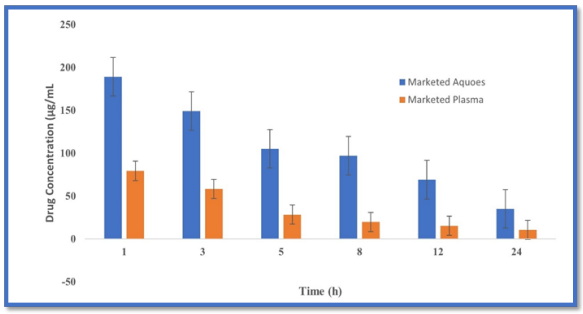

Figure 16: Comparison of marketed aqueous and plasma concentration of drug

favorable synergistic effects on the percentage of the entrapped drug when the three independent variables (X1, X2, X3) were increased individually while keeping other factors constant. According to the greater value of the X1 coefficient (11,84), the concentration of lipids is the primary influence on EE. For formulas F2 through F15, the increase in lipid concentration from 4 to 10% was significant when all other parameters were held constant. With its strong positive coefficient, increasing the surfactant concentration (X2) also increased drug %EE significantly (9.38) (Figure 3).

It is clear that SAA concentration synergizes impact VCZ EE in formulas F9, F14, F17, and F12 (SAA) when compared to formulae F7, F15, F10, and F11 (SAA). It is shown in Figure 3 that all three parameters have an impact on the VCZ %EE. However, the impact has suppressed higher concentrations of lipids, when %EE increased from 80.6 ± 0.61 to 89.2 ± 2.01%; after increasing X3 from low to high level. Due to high lipid concentrations that impede medication solubility in the lipid core, the formula's increased viscosity may be to blame. Increased sonication frequency overcame the significant increase in mixture viscosity caused by an increase in lipid concentration, which positively affected drug solubility within the lipid core and %EE when both variables were simultaneously increased (from 41.06 to 75.86%). The modest coefficient (2.25) shows that the % of VCZ entrapped rose from 49.2 to 89.2% when both factors were raised to a greater level, also showed a slight positive interaction impact on %EE. Surfactant concentration also exhibited no influence on the %EE at higher surfactant concentrations, which may be owing to the VCZ-solubilizing action of surfactant on the lipid core.[43]

Effect on ZP

This electro-kinetic potential is what affects the stability of colloidal dispersions, such as the SLNs formulations described above. ZP measures inter-particulate repulsion in the colloidal system, and it prevents agglomeration and reaggregation inside the phase. In most cases, the ZP is governed by the surfactant's chemical composition and the HLB of the solution. SLNs with a low ZP are prone to collapsing during storage, making them unstable. Having a ZP of 30 mV shows that a formula is stable in its physical state. As negatively charged corneal epithelial cells, surface charges in ocular medication delivery are crucial for corneal drug absorption.

As a result, the corneal morphology of cationic SLNs is altered by ionic interactions, resulting in longer conjunctival residence periods and more corneal penetration. The SLNs were treated with the charge-inducing substance stearyl amine throughout the preparation phase (based on the results of preliminary experiments) to enhance ZP. Lipophilicity means that the stearyl amine is confined inside the lipoprotein, and its substituted charged amine groups projecting outward act as an electrostatic repellent on the particle surface. There were ZP (R2) values from -22.5 ± 0.85 mV (F15) to -39.6 ± 0.28 mV for the produced VCZ-SLNs (F9) (Figure 4).

$$\text{zeta potential} = -25.56 +3.73A +1.59B -0.6067C -2.89AB +0.6875AC +1.49BC -1.57A2 +0.3876B2 -2.14C2$$

Only the model variables A, B, AB, BC, A2 and C2 had *p-values* 5% significance in the ANOVA, as shown in Table 5. Its larger coefficient value (6.07) when compared to other relevant factor coefficients in the polynomial equation, indicates that the surfactant concentration had a major (X2) and quadratic ($X2^2$) antagonistic influence on ZP. Although ZP had a primary and quadratic synergistic effect on the lipid concentration, their coefficient values in the regression equation suggested that they had a lesser influence. As lipid content increases, the particle's surface area increases to accommodate a bigger charge density, and therefore a higher ZP is achieved. In most cases, the closeness of ZP values in the experimental design matrix reflects the influence of stearyl amines on the surface charge of the produced SLNs. In a perturbation plot, surfactant concentration (X2) was shown to have the greatest impact on ZP compared to other factors.

ZP Analysis

This surface characterization method, known as the ZP, is helpful in determining the stability and surface charge of nanoparticulate systems. Electrostatic repulsion between particles of the same charge necessitates a substantial absolute negative or positive zeta potential value in colloidal dispersions. For physical stability, Table 2 shows that all formulations had negative potential values ranging from 22.5 to 39.5 mV, which is closer to the intended 40 mV for stearic acid concentration (0.3% w/v) (Figure 5).[45]

Solid state Characterization

FTIR Analysis

Secondarily, FTIR is utilized to confirm the crystalline shield's stability in SLNs. Lyophilized VCZ-laden SLNs containing Isotope-labeled VCZ were synthesized as shown in Figure 6. According to FTIR spectra, OH was stretched to 3200.09–3046.04 cm, C-N to 1510.28–1451.28 cm^{-1}, and C-F to 1587.44–1451.28 cm^{-1} in VCZ. Stearic acid has a C=O stretching IR absorption band that is 1.700 cm^{-1} in wavelength. Most of the FTIR spectra were absent except for the C=C aromatic and C-N aryl peaks at 1618.89 and 1281.86 cm^{-1}, respectively, which indicated that the SLNs and formulation had a substantial interaction (C-N aryl). Figure 6 shows the C-H stretch, the 1702.5 cm^{-1} C=O stretch, and the 1466.1 cm^{-1} C-H stearic acid peaks (C-H bend). Since the FTIR spectra showed most of the drug's characteristic peaks, VCZ had no effect on either the physical combination or the SLNs of PA and VCZ. The drug, SLS, and stearic acid combination showed no significant alterations in the spectra of the drug, lipids, polymers, or physical mixtures. There was no interaction between the polymer, lipids, and medicine. The OH and C-O stretching IR peaks created by ultrasonication were 3389 and 1086 cm^{-1}, respectively.[46] Tristearin and poloxamer 188 peaks at 1702 and 2935 cm^{-1} were clearly visible in the lyophilized nanoparticles (F3).

DSC

The melting and recrystallization characteristics of a material may be examined using DSC. The thermograms of DSC samples are shown in the Figure 7. The endotherm of VCZ, for example, is well defined at 132.04°C and the drug's fusion heat is 95.08 J/g, as shown by the thermogram. The melting point of stearic acid is 56.18°C, and its fusion heat is 157.19 J/g. The DSC thermogram clearly displays an endothermic peak at stearic acid's melting point of 60.32°C. The physical mixture's melting points of 140.52, 56.48, and 83.32°C were not altered when VCZ was mixed with stearic acid and SLS. SLNs (F3) showed a shift in the drug's melting point at 119.89ºC, but SLNs (F2) did not show this change (flat peak). In the SLNs, a flat peak indicated that the medication was scattered in an amorphous crystalline phase. It is possible that high temperatures and/or high-speed stirring might have an effect on the formulation development process. The DSC scan of SLNs showed an endothermic peak at 78°C. In the DSC curve, an endothermic peak at 164.64°C seemed to be depressed, which matched the melting point of SLN. The drug did not seem to dissolve at any time in the thermograms. There was evidence of an oil-based matrix around VCZ if the drug was determined to be in amorphous form. Because of the surfactant and fast quenching of the microemulsion, the medicine does not crystallize.[47]

Morphological Studies

Using SEM, most of the vesicles were discovered to be spherical. The lipid composition has a significant impact on the effectiveness of drug entrapment. An SEM image of SLNs shows consistent particle shape and size distribution in the revised formulation. Smooth and homogeneous surfaces were discovered on the lipid nanoparticle. Light surrounds smaller than 200 nm diameter particles, making them seem darker in TEM images (Figure 8). The nanoparticles were dispersed across the region without any agglomeration, as shown by TEM. Each nanoparticle was found to have a spherical shape, and the nanoparticles were distributed evenly. The SLNs particles were found to be evenly dispersed throughout the mixture. NLC particles that were uniform and spherical in shape were found to have the same effect as NLC particles that were not. In order to better understand how the SLNs' morphology and particle aggregation change over time, AFM studies were done. AFM measurements have shown that the SLNs are tightly packed together, resulting in larger-than-expected particle size. This SLN aggregation was connected to the kind of sample preparation employed for AFM imaging since the samples may not be completely dry. The same things happened to us. The aggregation of particles in lyophilized blank and lyophilized VCZ-loaded SLNs was larger than in other process samples. In terms of particle size, this is in agreement with what was found by DLS and TEM.[48]

In-vitro Drug Release Studies

Dialysis bags were used to determine the drug release pattern by using a mixture of methanol and PBS (pH 6.4) (30:70) as the diffusion medium to evaluate the drug release. The VCZ suspension and the VCZ-SLNs have different release patterns. As expected, VCZ suspension produced an immediate quick

release, but the initial release times for VCZ-SLNs were delayed by up to half an hour or one hour, respectively. The quick initial release in ocular solution and suspension may be due to VCZ-SLNs and VCZ suspension being exposed directly to diffusion medium. It has been suggested that the controlled release profile of VCZ-SLNs formulations might be used for topical medication administration.[49]

In-vitro Skin Permeation, Stripping, and Retentivity Studies

VCZ was found in receptor compartment of skin of rats 24 hours after application of any of the administered formulations. After 24 hours of tape stripping, it was discovered that VCZ recovered using VCZ-SLNs had the greatest VCZ recovery rate (169.5 ± 6.23 g/cm^2) (Figure 9, Table 2). It was 20.35 ± 2.95 g/cm^2 for VCZ suspension and 11.36 ± 1.29 g/cm^2 for VCZ-SLNs. A better treatment profile for diseases like superficial mycoses, which are found in the higher layers of the skin, may be developed based on these findings, which show that drugs are present there. Furthermore, a post-tape stripping skin receptivity investigation found that VCZ-SLNs had almost 8.32 fold higher skin retention than the other formulations (Table 6). Occlusion of the transepidermal water loss by SLNs, which enhances skin hydration and permeability, may be responsible for the retentivity profile. Bio actives in the top skin layers may also accumulate, limiting medication flow and establishing an effective reservoir for longer-lasting therapy of upper skin infections and illnesses.[50]

Corneal Hydration Studies

The normal moisture of the mammalian cornea is between 75 to 80%.[32] An increase in polymer content in solid lipid nanoparticles did not damage the eyes (Figure 10). There was no injury to the corneal tissue in the formulations developed by both processes, which had a corneal hydration value of between 76 to 79% (Figures 10, 11).[52]

Irritation Study *In-vitro*

A Study of the Moisture of the Cornea

The SLNs exhibited a corneal hydration level of 75.64 ± 1.38%, suggesting a healthy cornea. To be considered healthy, the cornea must have a moisture content of 74 to 86%. When compared to the control and SLNs, the corneal hydration of 91.79 ± 1.83% was statistically significant (p 0.05). Until the cornea recovers to its physiologically normal value, swelling and endothelial pumping remove surplus fluid from the cornea. In terms of dry weight (g/g), this equates to an average corneal moisture content of 74 to 86%. Hydration levels over 83–92% may be a cause of corneal edema, according to the American Academy of Ophthalmology.[52]

Histopathology

In contrast to controls (0.9% NaCl) and irritant (0.1N NaOH)-treated corneas, those treated with SLNs and irritants experienced damage to the epithelial layer and Bowman's layer separation (Figure 12). As a result, the formulation-treated cornea revealed minimal or mild edema compared to the irritating treatment. Corneal edema is caused by fluid entering the stroma in an uncontrolled or excessive way due to damage to the epithelial layer. As a result, the nanoformulation was found to be non-irritating (F-3).

HETCAM Assay

The HETCAM test, which has been demonstrated to be especially helpful for identifying moderately irritating substances, may be used to predict eye irritation properties accurately. Despite the delivery of the nanoformulation, the chorioallantoic membrane was unaltered (F3). As a result, the IS for F3 was zero, showing that the nanoformulation did not irritate the test subjects. This is in contrast to the irritant's IS value of 19, which was determined to be due to the first 0.5 minutes of bleeding and the second minute of lysis (Table 7). Showed how HETCAM changed over time as a result of different formulations (Figure 13).

In-vivo (Draize Test)

No irritation or structural changes were noticed one week after applying the SLNs solution to all three ocular areas (total score = 0). In other words, it is non-irritating, as shown by this. Eye irritation is kept to a minimum because of the formulation's pH range and physiological oils.

In-vivo Study

The pharmacokinetics of an enhanced nanoformulation (F3) of VCZ, including peak concentration (C_{max}), time to peak concentration (T_{max}, and AUC0–12) following ocular injection to rats' eyes were investigated (Table 7). Compared to the drug solution, the F3 exhibited a longer T_{max} (three hours), which showed that the nanoformulation had a longer-lasting impact C_{max} was also observed to be higher in the nanoformulation than in the traditional drug solution (1978.2456 ± 22.39 g/mL) (2851.3459 ± 14.29 g/mL). VCZ AUC0-t for F3 was 37.958 ± 24.09 g.h/mL, while AUC0-t: 411.947 g.h/mL was substantially greater than that of the suspension (AUC0-t: 47.152 ± 96.81 and AUC0: 2276.067 ± 108.73 g/h/mL, respectively) (Figure 14).

There was a significant difference in the concentration of VCZ in plasma and aqueous humor, which indicated that the patient had reduced nasolacrimal discharge, reducing the risk of systemic toxicity even more (Figure 15). Improved corneal absorption by colloidal carriers (SLNs) compared to pure drug solution may help support fewer drug losses to plasma. After one hour, the plasma drug concentration was larger than the aqueous humor concentration when VCZ suspension was utilized (Figure 16).

CONCLUSION

For the VCZ-SLNs formulas, the optimization procedure revealed a considerable impact of the chosen variables. VS and EE benefited greatly from high lipid concentrations, but VS and ZP suffered significantly from high concentrations of surface active substances. Sonication frequency has a major impact on VS. For example, measurements of the improved formula's physical properties showed that it had an excellent

ZP (-39.6 ± 0.28 mV) and a very high percentage of drug EE (89.2 ± 2.01%). For 10 hours, the drug's release profile was compatible with the recipe. P_{app} and J_{ss} found that corneal permeability had significantly improved. There were no morphological alterations or symptoms of irritation in the *ex-vivo* histopathology examinations that were performed. Strong evidence supports the efficacy and safety of intraocular administration of low quantities of VCZ-SLNs in the treatment of deep corneal fungal infections. Additionally, the scientists are examining the corneal permeation qualities of the improved VCZ-SLNs formula in rabbit eyes, as well as ocular tolerance and pharmacokinetic/pharmacodynamic features of the permeation process. An induced fungal infection will also be used to test the *in-vivo* antifungal activity of the improved VCZ-SLNs formula.

REFERENCES

1. Wissing SA, Kayser O, Müller RH. Solid lipid nanoparticles for parenteral drug delivery. Advanced drug delivery reviews. 2004 May 7;56(9):1257-72.
2. Kaur IP, Garg A, Singla AK, Aggarwal D. Vesicular systems in ocular drug delivery: an overview. International journal of pharmaceutics. 2004 Jan 9;269(1):1-4.
3. Araújo J, Gonzalez E, Egea MA, Garcia ML, Souto EB. Nanomedicines for ocular NSAIDs: safety on drug delivery. Nanomedicine: Nanotechnology, Biology and Medicine. 2009 Dec 1;5(4):394-401.
4. Hironaka K, Inokuchi Y, Tozuka Y, Shimazawa M, Hara H, Takeuchi H. Design and evaluation of a liposomal delivery system targeting the posterior segment of the eye. Journal of Controlled Release. 2009 Jun 19;136(3):247-53.
5. Mehnert W, Mäder K. Solid lipid nanoparticles: production, characterization and applications. Advanced drug delivery reviews. 2001 Apr 25;47(2-3):165-96.
6. Seyfoddin A, Shaw J, Al-Kassas R. Solid lipid nanoparticles for ocular drug delivery. Drug delivery. 2010 Oct 1;17(7):467-89.
7. Leonardi A, Bucolo C, Romano GL, Platania CB, Drago F, Puglisi G, Pignatello R. Influence of different surfactants on the technological properties and in vivo ocular tolerability of lipid nanoparticles. International journal of pharmaceutics. 2014 Aug 15;470(1-2):133-40.
8. Leonardi A, Bucolo C, Drago F, Salomone S, Pignatello R. Cationic solid lipid nanoparticles enhance ocular hypotensive effect of melatonin in rabbit. International journal of pharmaceutics. 2015 Jan 15;478(1):180-6.
9. Cavalli R, Gasco MR, Chetoni P, Burgalassi S, Saettone MF. Solid lipid nanoparticles (SLN) as ocular delivery system for tobramycin. International journal of pharmaceutics. 2002 May 15;238(1-2):241-5.
10. Gaudana R, Jwala J, Boddu SH, Mitra AK. Recent perspectives in ocular drug delivery. Pharmaceutical research. 2009 May;26:1197-216.
11. Bucolo C, Drago F, Salomone S. Ocular drug delivery: a clue from nanotechnology. Frontiers in pharmacology. 2012 Oct 25;3:188.
12. Yüksel N, Karataş A, Özkan Y, Savaşer A, Özkan SA, Baykara T. Enhanced bioavailability of piroxicam using Gelucire 44/14 and Labrasol: in vitro and in vivo evaluation. European journal of pharmaceutics and biopharmaceutics. 2003 Nov 1;56(3): 453-9.
13. Attama AA, Reichl S, Müller-Goymann CC. Diclofenac sodium delivery to the eye: in vitro evaluation of novel solid lipid nanoparticle formulation using human cornea construct. International journal of pharmaceutics. 2008 May 1;355(1-2):307-13.
14. Li X, Nie SF, Kong J, Li N, Ju CY. A controlled-release ocular delivery system for ibuprofen based on nanostructured lipid carriers. International journal of pharmaceutics. 2008 Nov 3;363(1-2):177-82.
15. Hippalgaonkar K, Adelli GR, Hippalgaonkar K, Repka MA, Majumdar S. Indomethacin-loaded solid lipid nanoparticles for ocular delivery: development, characterization, and in vitro evaluation. Journal of ocular pharmacology and therapeutics. 2013 Mar 1;29(2):216-28.
16. Yellepeddi VK, Palakurthi S. Recent advances in topical ocular drug delivery. Journal of Ocular Pharmacology and Therapeutics. 2016 Mar 1;32(2):67-82.
17. Dubald M, Bourgeois S, Andrieu V, Fessi H. Ophthalmic drug delivery systems for antibiotherapy—A review. Pharmaceutics. 2018 Jan 13;10(1):10.
18. Kammari R, Das NG, Das SK. Nanoparticulate systems for therapeutic and diagnostic applications. Emerging Nanotechnologies for Diagnostics, Drug Delivery and Medical Devices. 2017 Jan 1:105-144.
19. Ram DT, Debnath S, Babu MN, Nath TC, Thejeswi B. A review on solid lipid nanoparticles. Research Journal of Pharmacy and Technology. 2012;5(11):1359-1368.
20. Mishra D, Dhote V, Pradyumna M, Chourasia MK, Chaurasia M, Jain NK. Solid lipid nanoparticles: a promising colloidal carrier. Novel Carriers for Drug Delivery. 2014:278-301.
21. Alhagiesa AW, Ghareeb MM. The Formulation and Characterization of Nimodipine Nanoparticles for the Enhancement of solubility and dissolution rate. Iraqi Journal of Pharmaceutical Sciences (P-ISSN 1683-3597 E-ISSN 2521-3512). 2021 Dec 11;30(2):143-152.
22. El-Salamouni NS, Farid RM, El-Kamel AH, El-Gamal SS. Effect of sterilization on the physical stability of brimonidine-loaded solid lipid nanoparticles and nanostructured lipid carriers. International journal of pharmaceutics. 2015 Dec 30;496(2):976-83.
23. Khames A. Preparation and characterization of sildenafil loaded solid lipid nanoparticles: drug delivery system suitable for nebulization ahmed khames. Der Pharmacia Lettre. 2017;2107(9):3.
24. Ruckmani K, Sivakumar M, Ganeshkumar PA. Methotrexate loaded solid lipid nanoparticles (SLN) for effective treatment of carcinoma. Journal of nanoscience and nanotechnology. 2006 Sep 1;6(9-10):2991-2995.
25. Youshia J, Kamel AO, El Shamy A, Mansour S. Design of cationic nanostructured heterolipid matrices for ocular delivery of methazolamide. International journal of nanomedicine. 2012 May 17:2483-2496.
26. Wu C, Qi H, Chen W, Huang C, Su C, Li W, Hou S. Preparation and evaluation of a Carbopol®/HPMC-based in situ gelling ophthalmic system for puerarin. Yakugaku Zasshi. 2007 Jan 1;127(1):183-191.
27. Joshi M, Patravale V. Formulation and evaluation of nanostructured lipid carrier (NLC)–based gel of Valdecoxib. Drug development and industrial pharmacy. 2006 Jan 1;32(8):911-918.
28. Thangabalan B, Kumar PV. Analytical method development and validation of natamycin in eye drop by RP-HPLC. Asian J Pharm Clin Res. 2013;6(1):134-135.

29. Ali AH, Abd-Alhammid SN. Enhancement of solubility and improvement of dissolution rate of atorvastatin calcium prepared as nanosuspension. Iraqi Journal of Pharmaceutical Sciences (IJPS). (P-ISSN 1683 - 3597 E-ISSN 2521 - 3512): 2019 Dec 22;28(2):46-57.
30. Katara R, Majumdar DK. Eudragit RL 100-based nanoparticulate system of aceclofenac for ocular delivery. Colloids and surfaces B: biointerfaces. 2013 Mar 1;103:455-462.
31. Ghanshyam U, Patel P, Patel J. Formulation and characterization of solid lipid nanoparticles dry powder inhaler containing triamcinolone acetonide. International Journal of Research in Pharmacy and Chemistry. 2011;1(3):662-673.
32. Youshia J, Kamel AO, El Shamy A, Mansour S. Design of cationic nanostructured heterolipid matrices for ocular delivery of methazolamide. International journal of nanomedicine. 2012 May 17:2483-2496.
33. Hu FQ, Yuan H, Zhang HH, Fang M. Preparation of solid lipid nanoparticles with clobetasol propionate by a novel solvent diffusion method in aqueous system and physicochemical characterization. International journal of pharmaceutics. 2002 Jun 4;239(1-2):121-128.
34. Drais HK, Hussein AA. Rheological Investigation of Lipid Polymer Hybrid Nanocarriers for Oral Delivery of Felodipine (Conference Paper). Iraqi Journal of Pharmaceutical Sciences (P-ISSN 1683-3597 E-ISSN 2521-3512). 2021;30(Suppl.):9-15.
35. Yang M, Chen X, Wang Y, Yuan B, Niu Y, Zhang Y, Liao R, Zhang Z. Comparative evaluation of thermal decomposition behavior and thermal stability of powdered ammonium nitrate under different atmosphere conditions. Journal of hazardous materials. 2017 Sep 5;337:10-19.
36. Müller RH, Radtke M, Wissing SA. Solid lipid nanoparticles (SLN) and nanostructured lipid carriers (NLC) in cosmetic and dermatological preparations. Advanced drug delivery reviews. 2002 Nov 1;54:S131-55.
37. Natarajan J, Baskaran M, Humtsoe LC, Vadivelan R, Justin A. Enhanced brain targeting efficacy of Olanzapine through solid lipid nanoparticles. Artificial Cells, Nanomedicine, and Biotechnology. 2017 Feb 17;45(2):364-371.
38. Salim FF, Rajab NA. Formulation and Characterization of Piroxicam as Self-Nano Emulsifying Drug Delivery System. Iraqi Journal of Pharmaceutical Sciences (P-ISSN 1683-3597 E-ISSN 2521-3512). 2020 Jun 25;29(1):174-183.
39. Ritger PL, Peppas NA. A simple equation for description of solute release I. Fickian and non-fickian release from non-swellable devices in the form of slabs, spheres, cylinders or discs. Journal of controlled release. 1987 Jun 1;5(1):23-36.
40. Scadding GK, Tasman AJ, Murrieta-Aguttes M, Bachert C, Riperex Study Group. Mizolastine is effective and well tolerated in long-term treatment of perennial allergic rhinoconjunctivitis. Journal of international medical research. 1999 Nov;27(6):273-285.
41. Sebbag L, Allbaugh RA, Weaver A, Seo YJ, Mochel JP. Histamine-induced conjunctivitis and breakdown of blood–tear barrier in dogs: a model for ocular pharmacology and therapeutics. Frontiers in Pharmacology. 2019 Jul 9;10:752: 1–11.
42. SEYED YA, Shahidi F, Mohebbi M, Varidi M, Golmohammadzadeh SH. The effect of different lipids on physicochemical characteristics and staibility of phycocyanin-loaded solid lipid nanoparticles. *Iran J Food Sci Technol*. 2017;14(67):83–93.
43. Gupta S, Kesarla R, Chotai N, Misra A, Omri A. Systematic approach for the formulation and optimization of solid lipid nanoparticles of efavirenz by high pressure homogenization using design of experiments for brain targeting and enhanced bioavailability. Biomed research international. 2017 Jan 23;2017.
44. Seyfoddin A, Shaw J, Al-Kassas R. Solid lipid nanoparticles for ocular drug delivery. Drug delivery. 2010 Oct 1;17(7):467-89.
45. Negi JS, Chattopadhyay P, Sharma AK, Ram V. Development of solid lipid nanoparticles (SLNs) of lopinavir using hot self nano-emulsification (SNE) technique. European Journal of Pharmaceutical Sciences. 2013 Jan 23;48(1-2):231-9.
46. Hulse WL, Forbes RT, Bonner MC, Getrost M. The characterization and comparison of spray-dried mannitol samples. Drug development and industrial pharmacy. 2009 Jan 1;35(6):712-8.
47. Cavalli R, Caputo O, Carlotti ME, Trotta M, Scarnecchia C, Gasco MR. Sterilization and freeze-drying of drug-free and drug-loaded solid lipid nanoparticles. International journal of pharmaceutics. 1997 Mar 14;148(1):47-54.
48. Katara R, Majumdar DK. Eudragit RL 100-based nanoparticulate system of aceclofenac for ocular delivery. Colloids and surfaces B: biointerfaces. 2013 Mar 1;103:455-62.
49. Alkawak RS, Rajab NA. Lornoxicam-Loaded Cubosomes:-Preparation and In vitro Characterization. Iraqi Journal of Pharmaceutical Sciences (P-ISSN 1683-3597 E-ISSN 2521-3512). 2022 Jun 17;31(1):144-53.
50. Puglia C, Filosa R, Peduto A, De Caprariis P, Rizza L, Bonina F, Blasi P. Evaluation of alternative strategies to optimize ketorolac transdermal delivery. Aaps Pharmscitech. 2006 Sep;7:E61-9.
51. Peira E, Carlotti ME, Trotta C, Cavalli R, Trotta M. Positively charged microemulsions for topical application. International journal of pharmaceutics. 2008 Jan 4;346(1-2):119-23.
52. Monti D, Chetoni P, Burgalassi S, Najarro M, Saettone MF. Increased corneal hydration induced by potential ocular penetration enhancers: assessment by differential scanning calorimetry (DSC) and by desiccation. International journal of pharmaceutics. 2002 Jan 31;232(1-2):139-47.